Heliyon 10 (2024) e34586

Contents lists available at ScienceDirect

Heliyon

journal homepage: www.cell.com/heliyon

Research article

A cuproptosis-related lncRNAs signature predicts prognosis and reveals pivotal interactions between immune cells in colon cancer

Jingru Song [a,1], Dong Xie [b,1], Xia Wei [a], Binbin Liu [a], Fang Yao [a], Wei Ye [a,*]

[a] Department of Gastroenterology, Hangzhou TCM Hospital Affiliated to Zhejiang Chinese Medical University, Hangzhou, 310007, Zhejiang, China
[b] Shanghai University of Traditional Chinese Medicine, Shanghai, 201203, China

ARTICLE INFO

Keywords:
Colon cancer
Cuproptosis
lncRNAs
Prognostic signature
Immune microenvironment
Cell communication

ABSTRACT

Copper-mediated cell death presents distinct pathways from established apoptosis processes, suggesting alternative therapeutic approaches for colon cancer. Our research aims to develop a predictive framework utilizing long-noncoding RNAs (lncRNAs) related to cuproptosis to predict colon cancer outcomes while examining immune interactions and intercellular signaling. We obtained colon cancer-related human mRNA expression profiles and clinical information from the Cancer Genome Atlas repository. To isolate lncRNAs involved in cuproptosis, we applied Cox proportional hazards modeling alongside the least absolute shrinkage and selection operator technique. We elucidated the underlying mechanisms by examining the tumor mutational burden, the extent of immune cell penetration, and intercellular communication dynamics. Based on the model, drugs were predicted and validated with cytological experiments. A 13 lncRNA–cuproptosis-associated risk model was constructed. Two colon cancer cell lines were used to validate the predicted representative mRNAs with high correlation coefficients with copper-induced cell death. Survival enhancement in the low-risk cohort was evidenced by the trends in Kaplan–Meier survival estimates. Analysis of immune cell infiltration suggested that survival was induced by the increased infiltration of naïve $CD4^+$ T cells and a reduction of M2 macrophages within the low-risk faction. Decreased infiltration of naïve B cells, resting NK cells, and M0 macrophages was significantly associated with better overall survival. Combined single-cell analysis suggested that CCL5–ACKR1, CCL2–ACKR1, and CCL5–CCR1 pathways play key roles in mediating intercellular dialogues among immune constituents within the neoplastic microhabitat. We identified three drugs with a high sensitivity in the high-risk group. In summary, this discovery establishes the possibility of using 13 cuproptosis-associated lncRNAs as a risk model to assess the prognosis, unravel the immune mechanisms and cell communication, and improve treatment options, which may provide a new idea for treating colon cancer.

1. Introduction

Colorectal carcinoma (CRC) is the third most common oncologic fatal condition [1]. From 1990 to 2019, incidence of colorectal carcinoma increased twofold or greater in 157 out of 204 nations and regions. Mortality rates paralleled this surge, climbing from an estimated 518,126 (493,682–537,877) to 1.09 million (1.02–1.15 million) across 129 of the surveyed 204 territories [2]. CRC includes

* Corresponding author.
E-mail address: yewei7752@163.com (W. Ye).
[1] These authors contributed equally to this work.

https://doi.org/10.1016/j.heliyon.2024.e34586
Received 17 September 2023; Received in revised form 11 July 2024; Accepted 11 July 2024
Available online 14 July 2024

colon and rectal cancers [3]; however, these cancers differ in many ways, especially in terms of tumor biology, recurrence patterns, and treatment modalities [4]. Only a few effective therapeutic targets are available for treating patients with colon cancer. Treatment strategy and prognostic assessment of colon cancer have been intensely investigated. Therefore, exploring other possible therapeutic targets is crucial.

Copper is one of the most abundant basic transition metals in the human body [3]. Abnormalities in copper homeostasis may be caused by genetic mutations, aging, or environmental factors and produce various pathological sequelae, including cancer, inflammation, and neurodegeneration [5]. Dysregulation in copper homeostasis is implicated in oncogenesis, with tumor tissues exhibiting increased copper levels compared to nontumorous counterparts [6]. Elevated copper content within neoplastic tissues of the breast, pulmonary, digestive, oral, thyroid, hepatic, reproductive, and prostatic systems has been documented, implying a contributory role in tumorigenesis, vasculature formation, and tumor metastasis [7,8]. Limiting copper availability impairs cancer cell metabolism [9], and targeting copper metabolism is a potential target for cancer therapy [10]. Recent investigations indicate that copper-triggered apoptosis deviates fundamentally from established cell death pathways, including necroptosis, ferroptosis, and pyroptosis. This form of cell death is closely linked to the citric acid cycle through the modulation of protein lipoylation [11,12]. Specifically, in colorectal cancer, decreased glycolytic activity coupled with enhanced mitochondrial respiration indicates a growth-inhibitory environment, highlighting the significance of copper ion dynamics in prognostic evaluations and the development of novel cancer treatments [13]. Based on this new approach to cell death, the study sought to develop new methods of treatment and prognosis assessment for patients with colon cancer.

Long-noncoding RNAs (lncRNAs) are >200 bp in length and play important regulatory roles in controlling a wide range of cellular functions [14], including crucial immune processes such as the recruitment of immune cells, the identification and response to antigens, and the subsequent eradication of tumors [12,15–17]. lncRNAs also influence the growth and distant spread of various neoplastic cell types, establishing them as valuable markers for cancer diagnosis and prognosis [18–20]. Particularly in colorectal neoplasms, lncRNAs contribute to cellular invasion, dissemination, and secondary tumor formation [21,22]. Therefore, identifying key regulators of copper-induced cell death is an important step toward treating colon cancer. lncRNAs associated with cuproptosis present promising opportunities as novel biomarkers and as potential targets for developing innovative treatment strategies in colon cancer management.

The intricacies of cell mortality induced by copper in tumors are under investigation, with the specific contributions of lncRNAs related to cuproptosis in colon cancer yet to be elucidated. Leveraging bioinformatic techniques, this study probes into the functions of cuproptosis-connected lncRNAs within the context of colon cancer. Our research specifically focused on colon cancer and established a more robust predictive model for cuproptosis-related lncRNAs. Distinct from prior studies, our work delves deeply into the immune patterns and cellular communication associated with cuproptosis-related lncRNAs within the colon cancer milieu. Moreover, we provide cytological validation of the mRNAs interacting with these lncRNAs, reinforcing the biological relevance and potential therapeutic implications of our findings. This combination of a focused approach to treat colon cancer and the use of advanced analytical methods, along with cellular-level validation, underscores the novelty and significance of our study in cancer research.

2. Materials and methods

2.1. Collection of sample information

Our analysis encompassed a compendium of 452 colon carcinoma transcriptomes procured from the TCGA repository as of August 18, 2022 (https://portal.gdc.cancer.gov/). The selection criteria for these samples mandated comprehensive clinical details, including sex, age, and tumor staging. Both mutational profiles and additional clinical data, such as survival durations and statuses, were also retrieved from the TCGA database. Annotations for lncRNAs were sourced from the GENCODE database (https://www.gencodegenes.org/), and genes related to copper-mediated apoptosis were compiled based on prior literature [11].

2.2. Evaluating variance in expression of lncRNAs linked to cuproptosis

Employing a suite of analytical tools, specifically the “limma,” “dplyr,” “ggalluvial” and “ggplot2” packages, we constructed a Sankey diagram to elucidate the connections between genes implicated in cuproptosis and their associated lncRNAs. Pearson correlation analysis was conducted, setting the significance threshold at an absolute Pearson R value of >0.5 and a p-value of <0.001.

2.3. Cuproptosis-associated lncRNAs modeling construction and validation

Construction and Validation of Models for lncRNAs Associated with Cuproptosis.

TCGA’s colon cancer datasets were segregated into equal parts for training and testing purposes, establishing the framework for risk model development and subsequent performance assessment. LncRNAs with statistical significance ($p < 0.05$) correlating to overall survival (OS) outcomes were identified using univariate Cox regression analyses. To develop the predictive models while minimizing overfitting, we employed the “glmnet” R package for Cox regression and applied LASSO regression techniques to highlight the most predictive set of lncRNAs [23] The categorization of samples into training and validation sets facilitated the empirical assessment of the model’s precision. Risk scores were computed as follows:

$$\text{Risk Score} = \sum_{i=1}^{j} coeffient_i \times \text{expression}_i \quad (2)$$

Utilizing median risk scores and their associated coefficients, we stratified patient risks into dichotomous groups (low and high risks). OS and progression-free survival (PFS) prognostications were conducted using Kaplan–Meier (KM) survival estimates through the "survival" and "survminer" R functions. ROC (receiver operating characteristic curve) curves and AUC (area under the curve) metrics, derived from "survival," "rms," "pec," and "timeROC," were implemented to gauge model precision. The concordance index (C-index) was determined using a compilation of R resources, including "rms," "dplyr," "survival," and "pec," to assess prognostic accuracy. We utilized the C-index function from the pec package to compute time-dependent C-index values for each model. This function assesses the concordance of the survival models and produces C-index values over a sequence of evaluation times (0–10 years) using bootstrap resampling (B = 1000).

2.4. Establish and evaluate nomogram and calibration

We generated nomograms to visualize univariate and multivariate Cox analysis results by employing the "rms," "regplot," and "survival" functions within R. The fidelity of these graphical representations was examined, supplemented by calibration plots to further appraise the models.

2.5. Gene set enrichment analysis

The expression patterns of cuproptosis-associated lncRNAs for colon cancer samples were classified using the principal component analysis (PCA) to show the spatial distribution of different groups, and results were visualized using the "scatterplot3D" package in R software.

In addition, for differentially expressed genes (DEGs) in the low- and high-risk groups, Gene Ontology (GO) analysis and the Kyoto Encyclopedia of Genes and Genomes (KEGG) pathways for differential expression in both groups were performed using "org.Hs.eg.db," "clusterProfiler," and "enrichplot" packages in R software.

2.6. Tumor mutational burden analysis

We procured the tumor mutational burden (TMB) profiles from the TCGA repository and deployed the "maftools" toolkit within R to scrutinize and assimilate the data, subsequently discerning the disparities in TMB and corresponding survival prognostications across distinct risk stratifications.

2.7. Delving into tumoral immune characteristics and dysfunction exclusion metrics

In order to delineate the immune landscape, colon carcinoma expression datasets were processed through CIBERSORT (http://cibersort.stanford.edu/), applying a thousand simulations to quantify the prevalence of 22 immune cell variants [24]. Investigating the interplay between our prognostic model and immune cell infiltrates, we computed infiltration scores for each specimen using ssGSEA facilitated by the "gsva" package in R. KM analyses followed, revealing the association between the proportions of immune cells and patient outcomes.

For enhanced prognostication in the context of immune-based therapies, we retrieved the Tumor Immune Dysfunction and Exclusion (TIDE) metrics from the TIDE portal (http://tide.Harvard/University.edu), offering a superior predictive accuracy for immunotherapeutic responses when compared to conventional biomarkers [25,26].

2.8. Single-cell sequencing data processing and cell-communication analysis

Raw data for single-cell sequencing were obtained from the NCBI Gene Expression Omnibus (GEO) database, specifically the GSE110009 dataset, which includes 3585 cells from six patients with colon cancer. Quality control was performed by excluding cells with fewer than 200 or more than 2500 detected genes, fewer than 1000 or more than 10,000 UMIs (unique molecular identifier), and more than 5 % mitochondrial reads to remove low-quality cells and potential doublets. Data were normalized using the LogNormalize method and scaled to regress out unwanted variations, such as UMI counts and mitochondrial gene content. Dimensionality reduction was conducted using PCA, and UMAP (uniform manifold approximation and projection) was used for visualization. Clustering was performed using the Louvain algorithm. Doublets were predicted and filtered out using DoubletFinder. Immune cell-type deconvolution was performed using the CIBERSORT algorithm, and the results were visualized with violin plots. Annotation of cell-type clusters was done using the "celldex," "SingleR," and "Seurat monocle" packages and visualized on t-SNE plots [27,28]. CellChat was used to visualize cellular interactions, which included approximately 2000 ligand–receptor interactions [29].

2.9. Potential sensitive drug prediction

The drug sensitivity data used in our study were obtained from the Genomics of Drug Sensitivity in the cancer database. This

database provides comprehensive information on the response of various cancer cell lines to a wide range of anticancer drugs, measured in terms of the half-maximal inhibitory concentration (IC50). Drug IC50 values were used for drug sensitivity measurements [30]. In the final stages of our analysis to assess therapeutic efficacy against colon cancer, we estimated the IC50 of anticancer drugs using the "pRRophetic" algorithm in R. We analyzed whether there was a significant drug sensitivity to conventional treatments between the two groups. This was crucial for assessing the clinical relevance of the treatment options.

2.10. Cell viability assays and RT-qPCR of mRNA associated with lncRNAs in vitro

The starBase databases were used to predict interactions between lncRNAs and mRNAs [31,32]. Further refinement of our predictions hinged upon contrasting mRNA expression levels in tumorous versus healthy tissue obtained from the TCGA colon cancer database. We applied Spearman's rank correlation for a robust analysis of the interplay between lncRNAs and variably expressed mRNAs. Correlations were visualized using heatmaps generated by the ggplot2 package in R, enabling the selection of the lncRNA–mRNA pairs with the strongest associative signals.

Cell line cultivation involved two colon cancer variants, HCT116 and SW620, sourced from the Cell Bank of the Chinese Academy of Science. HCT116 cells thrived in McCoy 5A medium enriched with 10 % fetal bovine serum and 1 % penicillin–streptomycin solution, whereas SW620 cells thrived in Dulbecco's modified Eagle medium with the same supplementation. Cells in the logarithmic phase of growth were used for subsequent experimental investigations. Cell densities were determined at 5000 cells per well in 96-well culture plates and 2×10^5 per well in six-well plates. Subsequent experimental manipulations were performed when cells were at 60%–70 % confluence.

Cells were incubated with elesclomol (MCE, Shanghai, China) and $CuCl_2$ (Macklin, Shanghai, China) at the appropriate

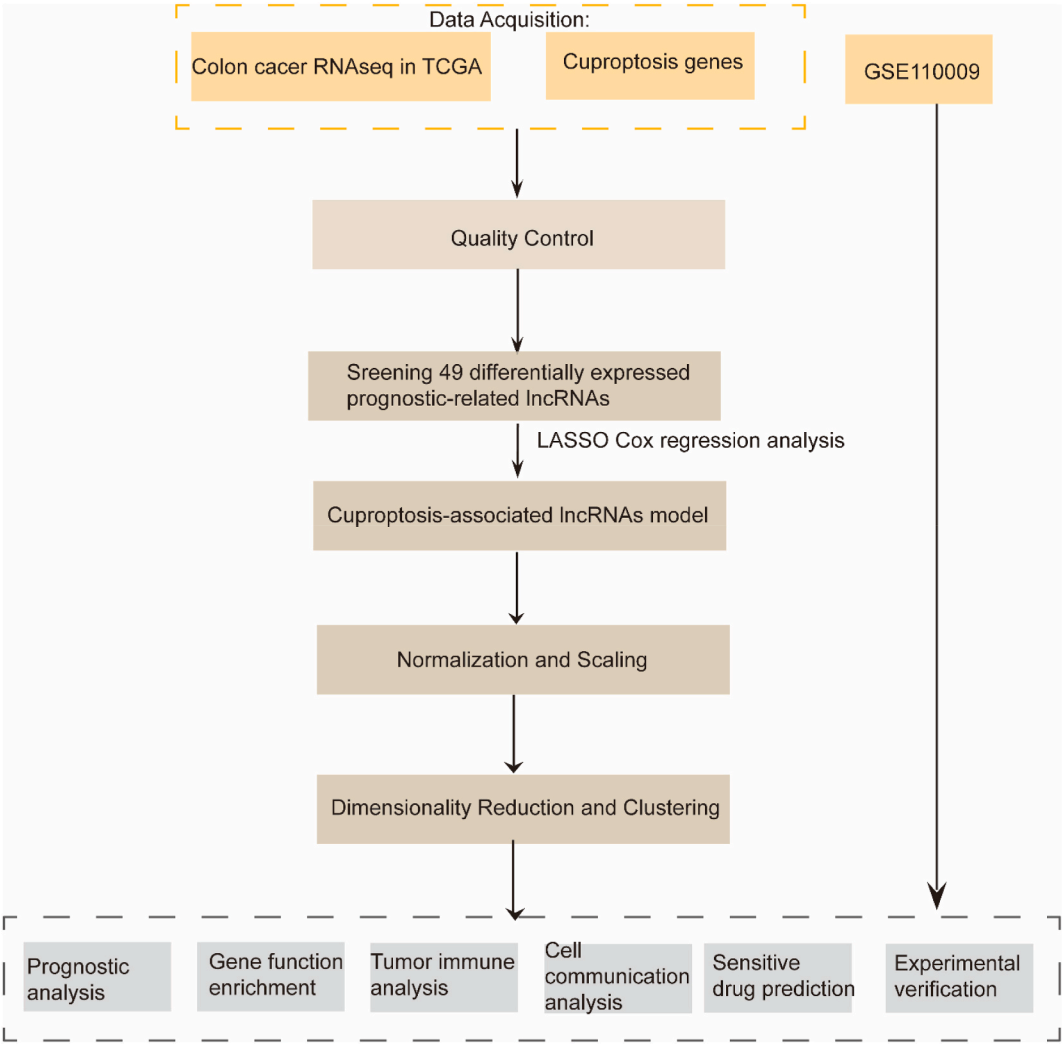

Fig. 1. Flow chart of study.

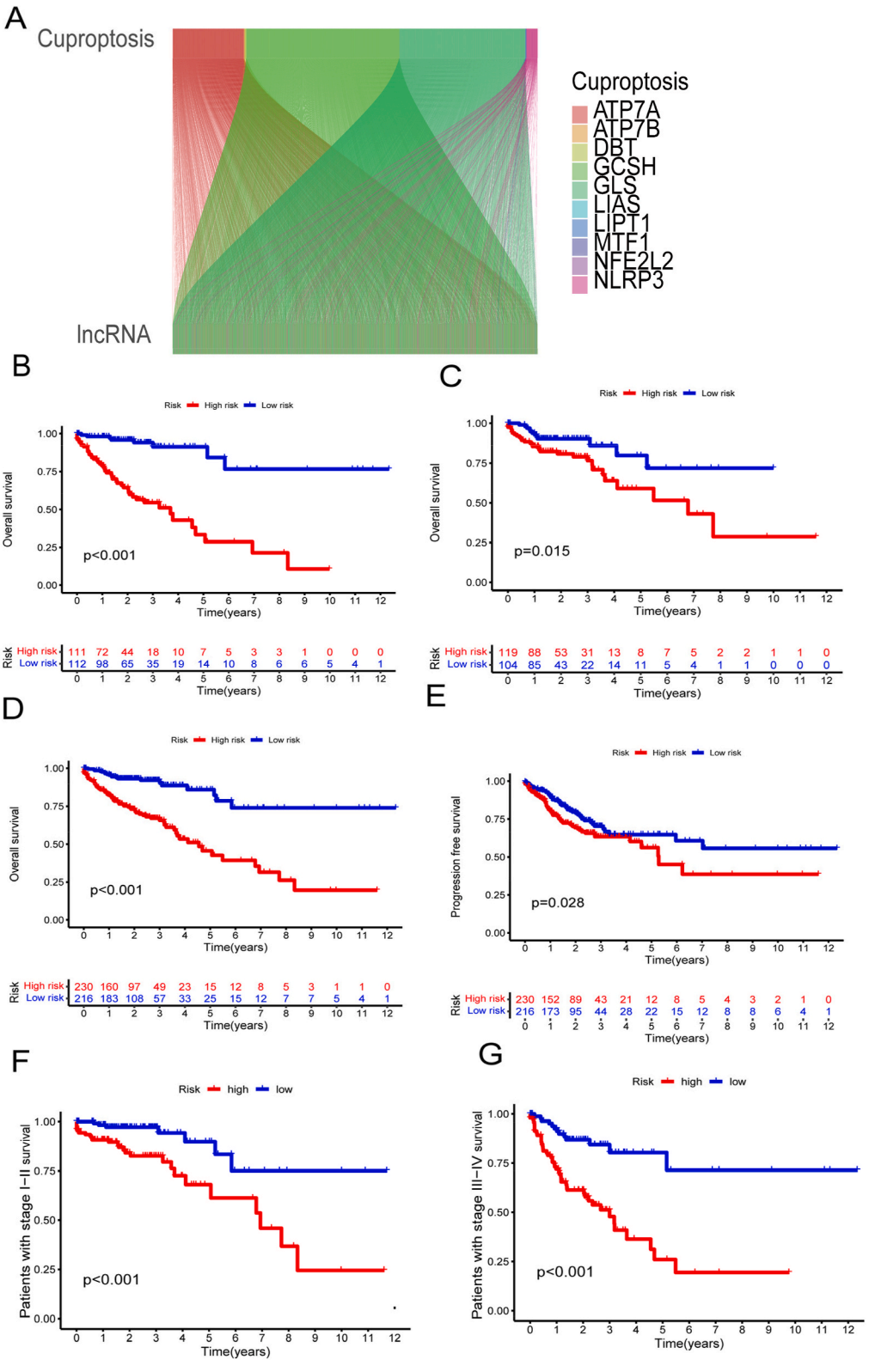

(caption on next page)

Fig. 2. Exploration of prognostic lncRNAs linked to cuproptosis in colon cancer. (A) Associations between cuproptosis-associated genes and lncRNAs. (B) KM survival curves depicting OS in the testing cohort. (C) KM survival curves for OS in the training cohort. (D) KM survival curves of OS in the total cohort. (E) KM survival curves of progression-free survival in the total cohort. (F, G) KM survival curves for low- and high-risk populations by stage.

concentrations. Cell viability assays were performed using the CCK8 assay (Topscience, Shanghai, China).

CuCl2 was used in our experiments as a source of copper ions (Cu^{2+}). $CuCl_2$ is commonly used in experimental studies on copper metabolism and toxicity. $CuCl_2$ provides a controlled and soluble source of copper ions, making it suitable for experimental use in cell culture systems.

We extracted total RNA utilizing the Trizol extraction method, as specified by Vazyme (Shanghai, China). cDNA synthesis was facilitated through reverse transcription protocols provided by Vazyme Biotech. For quantitative polymerase chain reaction analyses, we employed the ChamQ Universal SYBR qPCR Master Mix, also supplied by Vazyme, Shanghai, China. mRNA sequences are displayed in Supplementary Table 1. The reaction system had a volume of 10 μl, and the manufacturer's instructions were followed for all experimental procedures. Each group had five independent samples, with GAPDH serving as the control. The mRNA relative expression levels were determined using the $2^{-\Delta\Delta Ct}$ method.

2.11. Statistical analysis

In our study, all statistical computations were executed utilizing R (version 4.0.3). We assessed differences in continuous variables

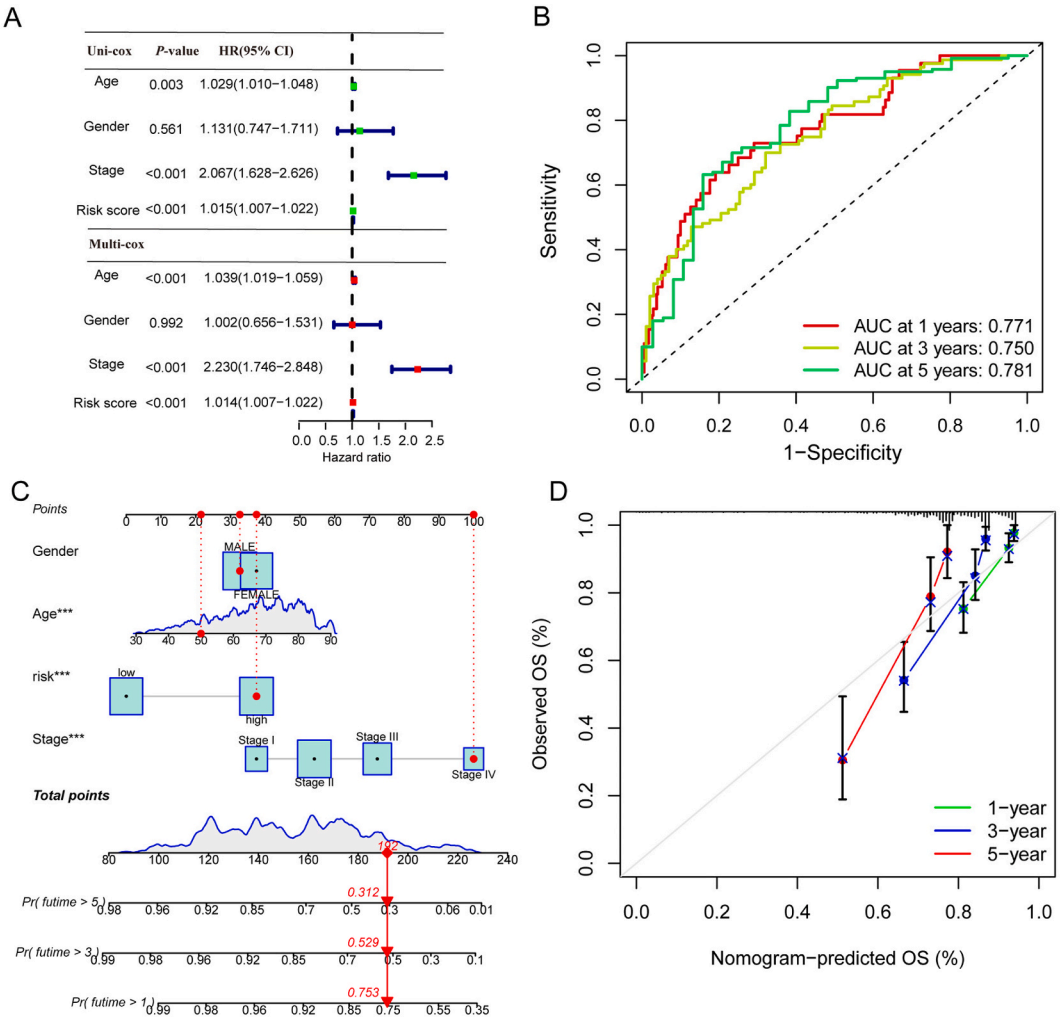

Fig. 3. Independence of cuproptosis-associated lncRNAs and developing a predictive nomogram. (A) Cox regression analyses, both univariate and multivariate. (B) Time ROC curves predicted at 1, 3, and 5 years intervals. (C) Construction of a nomogram for predicting patient outcomes. (D) Calibration curves validating the 1-, 3-, and 5-year OS predictions.

across groups via independent t-tests, whereas chi-square tests were employed for categorical data. We conducted KM and log-rank tests to support our univariate survival analyses. Moreover, we used Cox proportional hazards modeling for an in-depth multifactorial survival evaluation, considering p-values below 0.05 as statistically significant.

3. Results

3.1. Construction and cuproptosis-related lncRNA prognostic markers

This study's methodology is graphically depicted in Fig. 1.

We identified 1988 cuproptosis-associated lncRNAs that met the Pearson analysis criteria. The Sankey diagrams elucidate the correlation between genes implicated in cuproptosis and their corresponding lncRNAs (Fig. 2A). The 446 patients were split into testing (n = 223) and training groups (n = 223), and their clinical information is shown in Supplementary Table 2. The testing and training groups did not differ in any clinical characteristics.

Following univariate Cox regression analysis, 49 differentially expressed prognostic-related lncRNAs were used to choose. Furthermore, 13 cuproptosis-associated lncRNAs were identified from LASSO–COX regression. A risk score was formulated from the multivariate Cox regression model by combining the contributions of individual lncRNAs: risk score = AP000679.1 × (−2.708) + AC006111.2 × (−1.030) + AL513550.1 × (0.850) + AC005034.5 × (−0.649) + THCAT158 × (−0.841) + AC138646.1 × (0.458) + LINC00513 × (−0.296) + LCMT1-AS1 × (0.977) + AC245884.8 × (0.832) + CYP1B1-AS1 × (1.966) + AC103591.3 × (−0.260) + AC009041.3 × (−0.777) + AC106795.2 × (0.791) + LINC02257 × (0.829).

KM survival analyses revealed a statistical trend favoring improved survival in the low-risk group compared to the high-risk group. This pattern was consistently observed across the testing ($p < 0.001$), training ($p = 0.015$), and overall study populations (Fig. 2B–D). In addition, we found that the high-risk group exhibited diminished PFS compared with the low-risk group ($p = 0.028$) (Fig. 2E). Our findings also confirm that independent of the clinical stage, survival prospects were superior in the low-risk group ($p < 0.001$) (Fig. 2F and G). Conclusively, OS was notably reduced in the high-risk group across all segments of the study cohort.

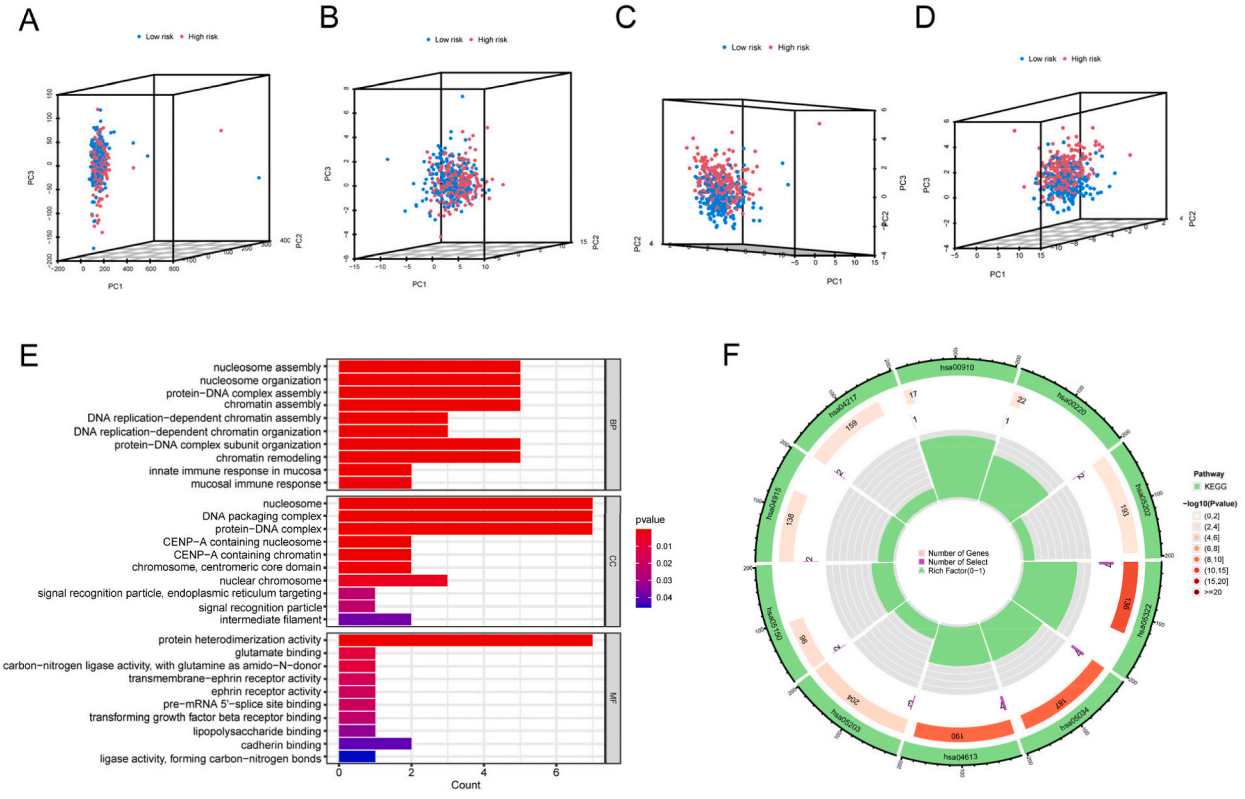

Fig. 4. Comprehensive analysis using PCA, GO, and KEGG. (A) General PCA overview of the gene pool. (B) Targeted PCA focusing on genes implicated in cuproptosis. (C) PCA of cuproptosis-related lncRNAs. (D) Dissection of lncRNAs related to risk assessment. (E) Exploration of gene function via GO enrichment. (F) KEGG pathway analysis.

3.2. Independence of cuproptosis-related lncRNAs as prognostic markers

Both univariate and multivariate Cox regression methodologies were applied to evaluate the forecast potential of our prognostic constructs (Fig. 3A). The univariate analysis revealed that age ($p = 0.003$, HR = 1.029), disease stage ($p < 0.001$, HR = 2.067), and risk score ($p < 0.001$, HR = 1.015) were prognostically relevant for patient mortality. Comparable trends were observed in the multivariate analysis, affirming the significance of age ($p < 0.001$, HR = 1.039), stage ($p < 0.001$, HR = 2.230), and risk score ($p < 0.001$, HR = 1.014). The AUC values reflected predictive reliability with scores of 0.771, 0.750, and 0.781 across 1-, 3-, and 5-year intervals, respectively (Fig. 3B).

3.3. Nomogram for cuproptosis-linked lncRNA prognostication

Based on this analytical framework, a nomogram was developed to predict OS at the 1-, 3-, and 5-year intervals (Fig. 3C). Calibration assessments of this nomogram displayed a high concordance with its prognostic predictions (Fig. 3D).

3.4. Comprehensive gene and enrichment profiling

PCA was systematically employed to profile the entire gene set, focusing on genes related to cuproptosis and lncRNAs for risk stratification (Fig. 4A–D). This approach identified 13 lncRNAs associated with cuproptosis as distinct markers distinguishing low- and high-risk cohorts.

Subsequent comparative analyses of the low-versus high-risk groups utilized GO and KEGG enrichment strategies. GO analysis highlighted the predominant roles of these genes in the innate and mucosal immune responses, along with glutamate binding activities (Fig. 4E). KEGG analysis mainly identified neutrophil extracellular trap formation, necroptosis, and transcriptional misregulation in cancer (Fig. 4F).

3.5. Mutational landscape associated with cuproptosis-linked lncRNA risk categories

An analysis of mutational prevalence highlighted *APC, TP53, TTN, KRAS, PIK3CA, MUC16, SYNE1, FAT4, ZFHX4, and RYR2* as the

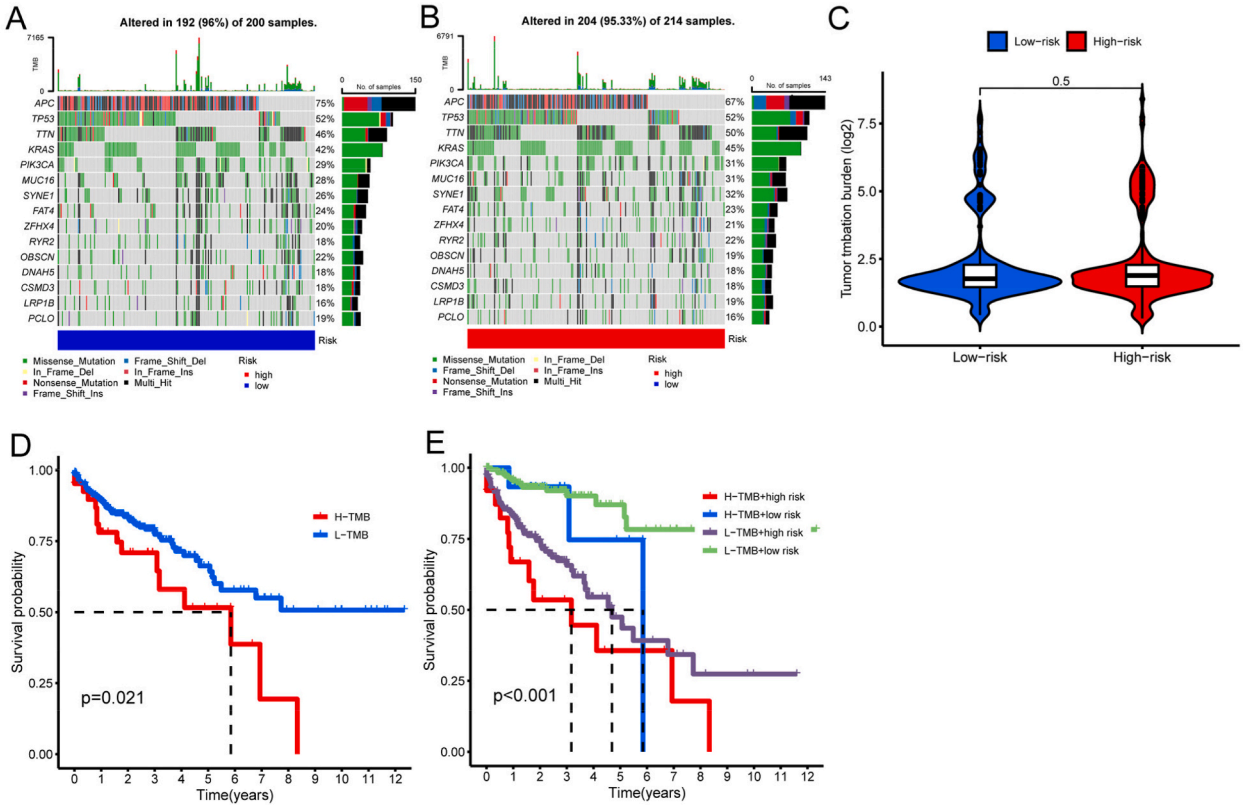

Fig. 5. Tumor mutational burden (TMB) of low- and high-risk groups. (A) Visualization of TMB in select pivotal genes for the low-risk subset. (B) TMB portrayal for predominant genes in the high-risk category. (C) Comparative TMB analysis across risk spectrums. (D) Survival projections stratified by TMB risk factors. (E) Integrated TMB and survival prognosis charts.

most frequently altered genes (Fig. 5A and B). However, the TMB did not show significant variation between the risk-defined groups (Fig. 5C). Notably, patients characterized by high TMB in the high-risk group correlated with poorer survival outcomes (Fig. 5D and E).

3.6. Immune profile and immunotherapeutic response prediction

Analysis of immune cell composition revealed differential infiltration levels between the low- and high-risk groups, with a higher infiltration of naïve $CD4^+$ T cells in the low-risk group and increased presence of M2 macrophages in the high-risk group (Fig. 6A). Fig. 6B illustrates the distribution of 22 immune cell types, as determined by CIBERSORT. A lesser infiltration of naïve B cells, resting NK cells, and M0 macrophages was associated with a significant enhancement in OS (Fig. 6C–E). The TIDE metric suggested a more

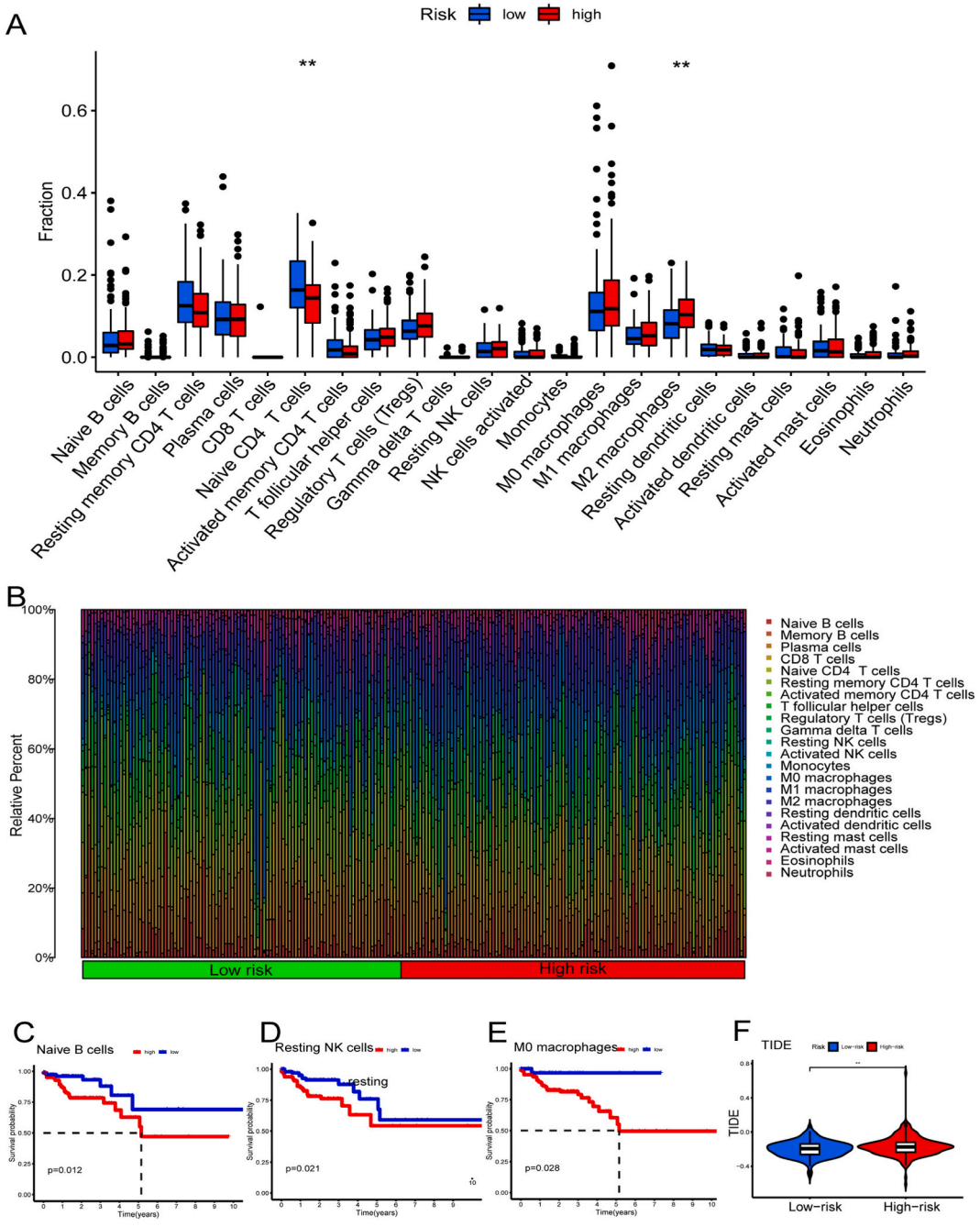

Fig. 6. Tumor immune microenvironment mapping of colon cancer. (A) The correlation of risk scores with 22 immune cells. (B) Relative abundance of 22 immune cells. (C–E) Kaplan-Meier plots correlating immune cell proportions with survival outcomes. (F) TIDE score for differing risk tiers.

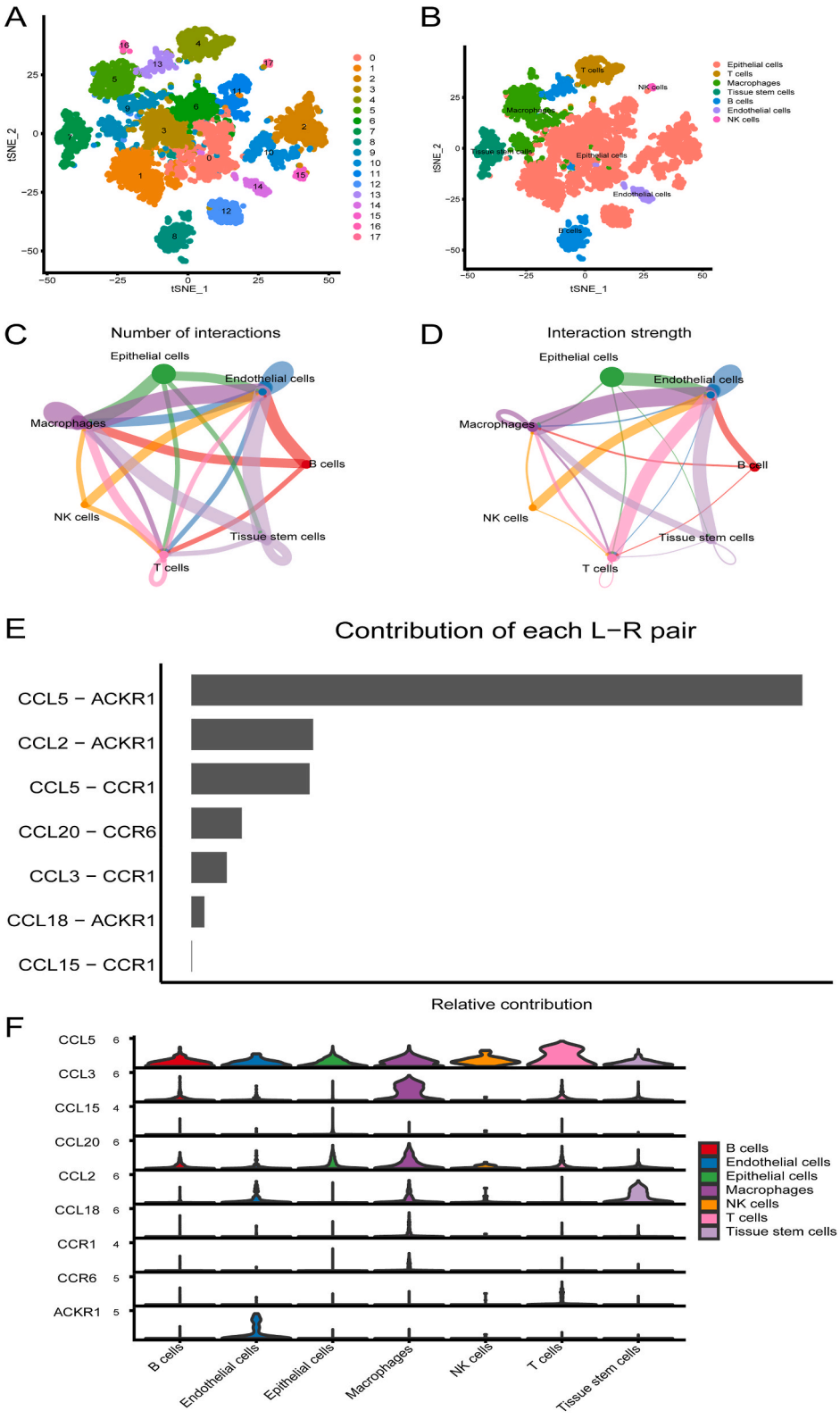

Fig. 7. Immune cell types and cell-communication network diagram. (A, B) All 17 cell-type clusters were annotated by CellMarker, according to the composition of the marker genes. (C, D) Quantification and intensity assessment of cellular communication channels. (E) Dynamic mapping of immune cell dialogues. (F) The distribution of expression level of signal genes.

favorable immunotherapeutic response in the low-risk group (Fig. 6F) [25].

3.7. Identification of different types of immune cells in colon cancer cell-communication analysis

The t-SNE algorithm is based on the SNE framework [33], which could recover well-separated clusters [34]. Based on the cell-type signatures, the analysis identified seven cell types, notably T cells, macrophages, B cells, and NK cells. (Fig. 7A and B). Furthermore, we examined the number and strength of significant receptor–ligand interactions between different cell types to predict intercellular communication (Fig. 7C and D). The results indicate a close link between epithelial cells, endothelial cells, macrophages, NK cells, T cells and other cell populations. These include pathways such as CCL, CALCR, ANGPTL, BMP, and the complement signaling pathway network. Central to these interactions were ligand–receptor pairs such as CCL5−ACKR1, CCL2−ACKR1, CCL5−CCR1, CCL20−CCR6, CCL3−CCR1, CCL18−ACKR1, and CCL15−CCR1 (Fig. 7E). In our study, the distribution of genes linked to signaling within the identified pathways was charted (Fig. 7F). We observed that CCL5 was predominantly produced by an array of cells, including T cells, macrophages, B cells, while its associated receptor, CCL3, was primarily active in macrophages and lymphocytes. The expression of CCL15 was concentrated in epithelial cells, with CCL20, its interacting receptor, being extensively present across a spectrum of cells such as macrophages and endothelial cells. CCL2 is mainly expressed on endothelial cells, macrophages, and tissue stem cells, and the corresponding receptor CCL18 is mainly expressed on macrophages. CCR1 is mainly expressed on macrophages, whereas CCR6 is mainly expressed on T cells, with their shared receptor ACKR1 prevalent in endothelial cells.

3.8. Therapeutic drug sensitivity

Drug sensitivity assessment revealed distinct IC50 values among the low- and high-risk groups. Notably, drugs such as cisplatin, CEP-701, and salubrinal demonstrated greater efficacy in the high-risk group, indicating an increased susceptibility of these cells to the therapeutic agents. The risk score was inversely proportional to the IC50 (Fig. 8A–C).

3.9. Experimental verification

Our study provided an in-depth analysis of the relationships between lncRNAs and mRNAs in the context of cancer. The volcano plot in Fig. 9A demonstrated mRNA differential expression analysis. Significantly upregulated genes are shown in red and clustered mainly on the right, indicating positive-fold changes. Conversely, significantly downregulated genes are shown in blue and clustered on the left, indicating negative-fold changes. A heatmap revealed the correlation strengths, with the most significant lncRNA–mRNA pairs being AC245884.8–*MSH5*, THCAT158–*CACNA2D1*, AC006111.2–*MSH5*, CYP1B1–AS1-*CLMP*, LINC02257–*CLMP*, LINC00513–*GTF2IRD1*, and AL513550.1–*MSH5* (Fig. 9B–Supplementary Table 3). Given the crucial role of copper-induced tumor cell death [11,35], we investigated the potential of copper therapy to enhance its destructive effect on tumors. To verify this, we conducted biological experiments using two colon cancer cell lines. Our findings demonstrate that the drug acting as a copper carrier exhibited cytotoxic effects on cells after 12 h in the presence of $CuCl_2$ (Fig. 9 C, D) However, no notable impact occurred when the drug was used alone. This observation supports the notion of copper-induced tumor cell death, which is consistent with previous literature [36]. In addition, we predicted the target genes related to lncRNAs with biological functions in our obtained lncRNA model. Through Spearman analysis, we obtained the four most strongly associated genes: *MSH5*, *CLMP*, *CACNA2D1*, and *GTF2IRD1*. In our in vitro cell experiments, copper-enhanced therapy promoted the expression of tumor suppressor CLMP (Fig. 9 G, H) and the downregulation of expression of *MSH5* (Fig. 9 E, F), *CACNA2D1* (Fig. 9 I, J), and *GTF2IRD1* (Fig. 9 K, L) in HT116 and SW620 cells.

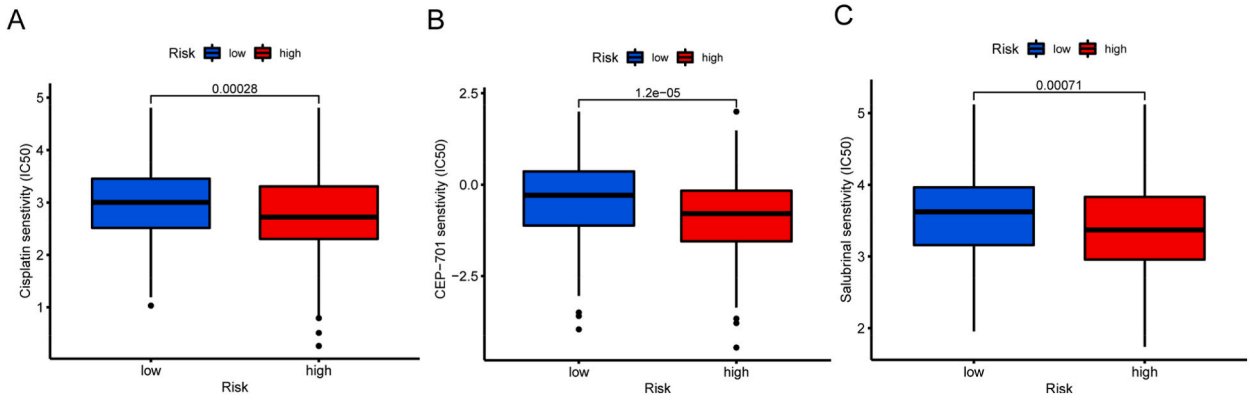

Fig. 8. Correlation of drug efficacy with low- and high-risk groups in colon cancer. (A) Cisplatin, (B) CEP−701, and (C) salubrinal.

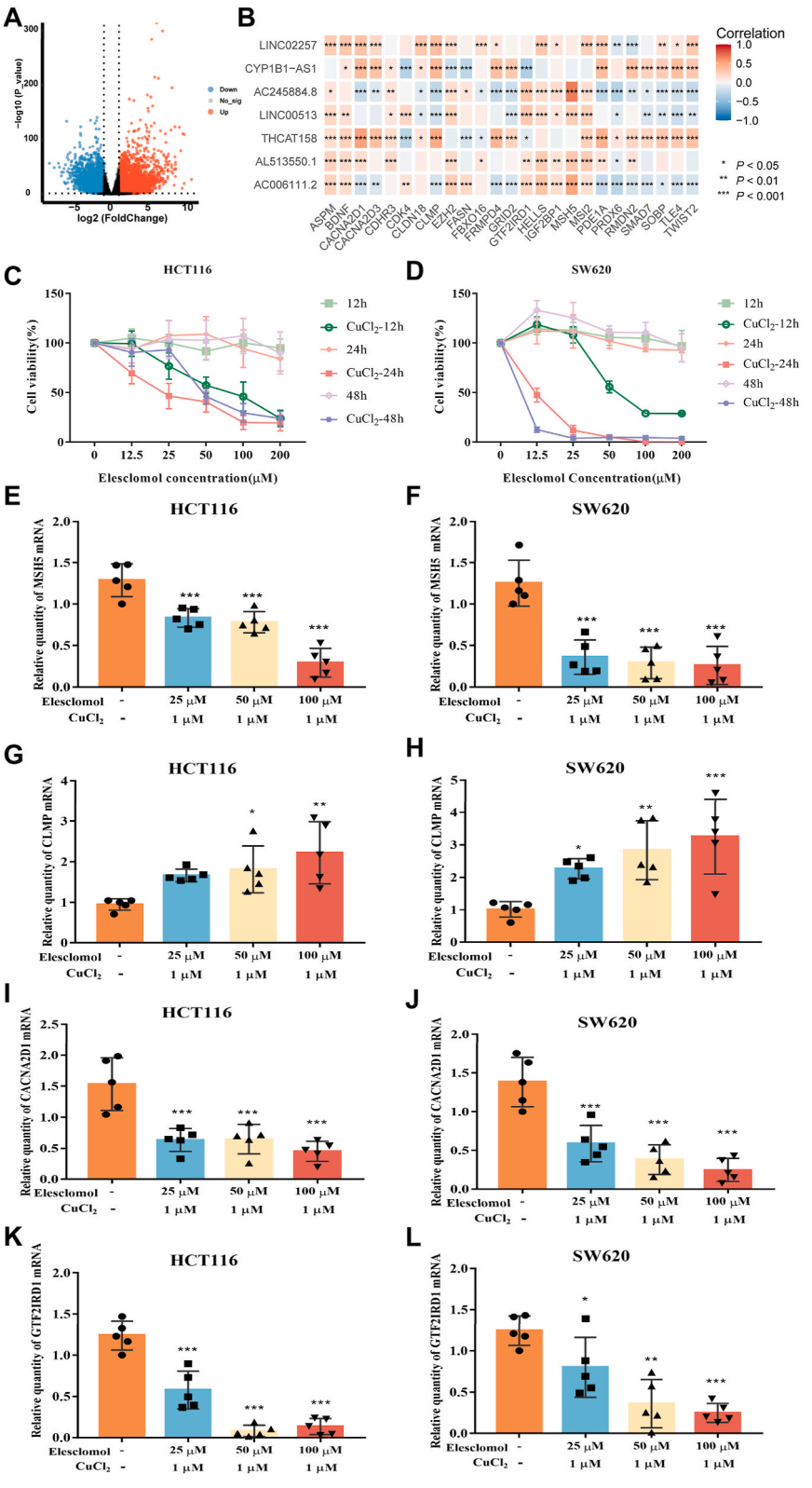

(caption on next page)

Fig. 9. (A) Volcano plot showing differential mRNA in tumor and normal groups. (B) Thermal imagery capturing the interactions between lncRNAs and mRNAs, annotated with statistical relevance by $*p < 0.05$, $**p < 0.01$, $***p < 0.001$. (C) Viability of HCT116 cells after treatment with elesclomol ± 1 μM of indicated metal. (C) Viability of SW620 cells after treatment with elesclomol ± 1 μM of indicated metal. (E, F) Relative quantity of *MSH5* mRNA In HCT116 and SW620 cells after treatment with elesclomol ± 1 μM $CuCl_2$ for 24 h. (G, H) Relative quantity of *CLMP* mRNA In HCT116 and SW620 cells after treatment with elesclomol ± 1 μM $CuCl_2$ for 24 h. (I, J) Relative quantity of *CACNA2D1* mRNA In HCT116 and SW620 cells after treatment with elesclomol ± 1 μM $CuCl_2$ for 24 h. (K, L) Relative quantity of *GTF2IRD1* mRNA In HCT116 and SW620 cells after treatment with elesclomol ± 1 μM $CuCl_2$ for 24 h. Mean ± SD,n = 5, $***p < 0.001$.

4. Discussion

Colon cancer treatment remains highly challenging despite the application of surgery and chemoradiotherapy. A detailed study of copper metabolism describes its close relationship with tumor origin and developmental stage [37]. Copper levels are higher in tumor cells than in normal cells [38,39]. Copper-deficiency therapies prevent tumor progression in clinical trials [40], and anticopper drugs have shown promising anticancer effects [41,42]. The accumulation of copper within cells leads to the assembly of mitochondrial lipid-acylated proteins and the depletion of Fe–S clusters, ultimately resulting in a specialized form of cell death known as cuproptosis [11]. These studies have raised new hopes for improved cancer treatment, and the advent of cuproptosis may produce a paradigm shift in the landscape of cancer treatment.

Recently, lncRNAs have received considerable attention in tumor development and progression [43–47]. Herein, we identified a set of 13 lncRNAs associated with cuproptosis that serve as predictors of OS in patients with colon cancer, including AP000679.1, AC006111.2, AL513550.1, AC005034.5, THCAT158, AC138646.1, LINC00513, LCMT1-AS1, AC245884.8, CYP1B1-AS1, AC103591.3, AC009041.3, AC106795.2, and LINC02257. Among these, LINC00513 is a new robust regulator for the interferon-signaling pathway that promotes disease progression and is associated with immune disorders [48]. Previous studies have constructed competing endogenous RNA networks containing AC245884.8 to reveal prognostic lncRNAs associated with immune infiltration in CRC [49]. CYP1B1-AS1 plays a regulatory role in immune activity and tumor progression [36,50–52]. In addition, LINC02257 is critical for carcinogenesis and significantly affects survival in patients with colon cancer [53–55]. However, few reports are available on AP000679.1, AC006111.2, AL513550.1, AC005034.5, THCAT158, AC138646.1, LCMT1-AS1, AC103591.3, AC009041.3, and AC106795.2. Therefore, these cuproptosis-associated lncRNAs warrant further investigation.

We built a cuproptosis-associated lncRNA prediction model that shows good accuracy in OS prediction. The PCA demonstrated that these particular lncRNAs are significant markers in distinguishing between patients with lower and higher risk profiles. Furthermore, the DEG analysis revealed a predominance of genes involved in immune response pathways, including those linked to neutrophil extracellular traps and necroptotic processes. Copper is essential for the maintenance of cellular and humoral immunities [56]. Consequently, we analyzed the TMB and immune phenotypes within the tumor microenvironment. Disparities were observed in the prevalence of naïve $CD4^+$ T cells and M2 macrophages when comparing immune infiltration in patients of different risk levels. The presence of naïve T cells within the tumor microenvironment suggests a retardation in tumor development, with their evolution into active effector cells aiding in tumor eradication [57]. Aging of the immune system, or immunosenescence, is identified by a reduction in naïve T cells and a decrease in $CD4^+$ and $CD8^+$ T-cell efficacy, which can diminish the immune system's capacity to combat tumors [58]. M2 macrophages are immunosuppressive and protumorogenic and can promote tumor angiogenesis and proliferation [59]. Subsequently, we observed a correlation between the presence of certain immune cells within tumors and patient outcomes. Notably, PD-L1, identified on naïve B cells marked by $CD19^+$, $CD80^+$, $CD86^+$, MHC-II+, $CD44^+$, and $CD69^+$, contributes to tumoral progression by impairing the activity of effector T cells [60,61]. Resting NK cells are generally less lytic against target cells and cannot recognize tumor cells for efficient killing [62], which indicates weak antitumorigenic immunity [63]. M0 macrophages can aggregate in tumor tissue and stimulate tumor growth [64], and their presence can predict poor survival outcomes [65]. Similarly, M0 macrophages were upregulated in tumors, suggesting an association with metastasis and progression in CRC [66]. Moreover, lower scores on the TIDE scale correlated with improved responses to immunotherapy in those at lower risk [25].

We updated CellChat by selecting receptor–ligand pairs corresponding to DEGs across risk strata. Particularly active were combinations such as CCL5–ACKR1 and CCL2–ACKR1. ACKR1, known for its nonspecific binding to a range of inflammatory CC and CXC chemokines, including CCL2 and CCL5 [67], was implicated in this network. ACKR1 was the causal link between reducing tumor growth, metastasis, and intensity of inflammatory reactions [68,69]. Tumor cells express CCL5 receptors, and serum CCL5 levels are closely related to tumor progression and prognosis in patients with gastric cancer and CRC [70]. CCL2–ACKR1, which has promalignant and proinflammatory effects [71], promotes the transfection of monocytes in inflammatory tissues [72]. CCR1 and its ligand CCL5 have been associated with cancer cell invasion and metastasis [73,74]. Typically produced by activated macrophages, CCL5 is implicated in promoting T-cell infiltration, although there is evidence to suggest that it also plays a role in immune evasion tactics [75]. CCL5/CCR1 participates in macrophage and NK migration and T-cell–DC interactions [76].

Studies have shown that MSH5 [77,78] was highly correlated with poor prognosis of tumors. Mutations in DNA repair genes at the *MSH5* locus are suggested to be associated with the emergence of lung and colorectal malignancies. Elevated *MSH5* expression correlates with increased risk of adverse outcomes in patients with cancer. Additionally, *CACNA2D1* expression is associated with stroma [79], influencing the progression and microenvironment of colon cancer by regulating fibroblasts. This correlation suggests its potential as a biomarker for disease progression and a novel target for treatment strategies. *CLMP* plays a pivotal role in mitigating cancer progression by orchestrating the growth of colonic epithelial cells and acting as a tumor inhibitor [80]. The influence of *CLMP* on IEC proliferation is mediated by its interaction with the mTOR–Akt–β-catenin signaling cascade, IEC suggesting its integral role in cellular homeostasis and tumor suppression. *CLMP* recruits β-catenin to the cell membrane, independent of cadherin proteins, thereby

suppressing CRC tumorigenesis and growth [81]. *GTF2IRD1* is highly upregulated in tumor tissues and adjacent tissues, and its expression is negatively correlated with the infiltration and antitumor activity of TILs and closely related to poor prognosis of tumors [82], with overexpression in neoplastic and surrounding tissues. Studies revealed that *GTF2IRD1* is implicated in the regulation of genes linked to the cell cycle [83]. This is a potential targeted link between lncRNAs and the intrinsic biological functions of tumors.

Cuproptosis is recognized as a new type of cell death that has gained widespread attention. Furthermore, some lncRNAs can impact cancer evolution in several ways. However, untapped opportunities exist for exploring regions between cuproptosis-associated genes and lncRNAs. Herein, we constructed a risk model using 13 cuproptosis-associated lncRNAs to forecast outcomes for patients with colon cancer and examined the relationship between mutations, immune infiltration levels, and cell–cell communication. This study has some limitations. First, TCGA data is limited and a broader dataset is needed to validate the model of the cuproptosis-related lncRNAs. Second, the mechanism of these cuproptosis-related lncRNAs is poorly elucidated. Their role in shaping the progression of tumor microenvironment and intercellular communication requires further study. Finally, more experimental validation is needed to comprehensively interpret the risk score model and treatment effects. These results provide direction for future therapeutic efforts.

5. Conclusions

This study establishes the possibility of using 13 cuproptosis-associated lncRNAs as a risk model to assess the outcomes, unravel the molecular mechanisms, and improve treatment options for colon cancer, which may have further clinical applications. Our study constructed a new model of 13 lncRNAs related to cuproptosis that may serve to predict the outcomes of patients with colon cancer. Insights from this model also pave the way for identifying new therapeutic avenues. Screening for anticancer drugs sensitive to copper may enhance patient benefits. The biological functions of the cuproptosis-related lncRNAs need to be further verified.

Funding

This work was supported by Hangzhou Medical Key Cultivation Discipline (Spleen and Gastroenterology, No. 2020SJZDXK13), Hangzhou Health and Health Commission (A20230658), and Provincial Central Management Bureau Heritage Innovation Talent Project (2024ZR121).

Ethics declarations

Informed consent was not necessary for this study as the data were derived from publicly available databases.

Institutional review board statement

The analysis of lncRNAs linked to cuproptosis in colon cancer utilized data from publicly available databases. Ethical consent for the patient information within the TCGA and GEO databases was duly acquired in prior studies. Our investigation relied on data that was already compiled and routinely gathered, ensuring that our research adhered to established ethical standards without any conflicts of interest.

Informed consent statement

Documentation confirming informed consent for publication has been secured from the participants involved.

Data availability statement

All datasets used for this study are accessible through online databases such as TCGA and GEO, providing a basis for replication and further research by the scientific community TCGA https://portal.gdc.cancer.gov/) and GEO (https://www.ncbi.nlm.nih.gov/geo/query/acc.cgi?acc=GSE110009).

CRediT authorship contribution statement

Jingru Song: Writing – original draft, Methodology. **Dong Xie:** Investigation, Conceptualization. **Xia Wei:** Data curation. **Binbin Liu:** Formal analysis. **Fang Yao:** Project administration. **Wei Ye:** Writing – review & editing, Funding acquisition.

Declaration of competing interest

The authors declare that they have no known competing financial interests or personal relationships that could have appeared to influence the work reported in this paper.

Appendix A. Supplementary data

Supplementary data to this article can be found online at https://doi.org/10.1016/j.heliyon.2024.e34586.

References

[1] Global burden of 369 diseases and injuries in 204 countries and territories, 1990-2019: a systematic analysis for the Global Burden of Disease Study 2019, Lancet (London, England) 396 (10258) (2020) 1204–1222.
[2] Global, regional, National burden of colorectal cancer and its risk factors, 1990-2019: a systematic analysis for the Global Burden of Disease Study 2019, Lancet Gastroenterol. Hepatol. 7 (7) (2022) 627–647.
[3] Q. Zhao, F. Hu, Z. Xiao, M. Li, X. Wu, Y. Zhao, Y. Wu, J. Yin, L. Lin, H. Zhang, L. Zhang, C.H. Cho, J. Shen, Comprehensive molecular profiling of the B7 family in gastrointestinal cancer, Cell Prolif. 51 (5) (2018) e12468.
[4] S. Paschke, S. Jafarov, L. Staib, E.D. Kreuser, C. Maulbecker-Armstrong, M. Roitman, T. Holm, C.C. Harris, K.H. Link, M. Kornmann, Are colon and rectal cancer two different tumor entities? A proposal to abandon the term colorectal cancer, Int. J. Mol. Sci. 19 (9) (2018).
[5] G. Gromadzka, B. Tarnacka, A. Flaga, A. Adamczyk, Copper dyshomeostasis in neurodegenerative diseases-therapeutic implications, Int. J. Mol. Sci. 21 (23) (2020).
[6] S. Blockhuys, E. Celauro, C. Hildesjö, A. Feizi, O. Stål, J.C. Fierro-González, P. Wittung-Stafshede, Defining the human copper proteome and analysis of its expression variation in cancers, Metallomics : Integrat. Biometal Sci. 9 (2) (2017) 112–123.
[7] P. Lelièvre, L. Sancey, J.L. Coll, A. Deniaud, B. Busser, The multifaceted roles of copper in cancer: a trace metal element with dysregulated metabolism, but also a target or a bullet for therapy, Cancers 12 (12) (2020).
[8] E.J. Ge, A.I. Bush, A. Casini, P.A. Cobine, J.R. Cross, G.M. DeNicola, Q.P. Dou, K.J. Franz, V.M. Gohil, S. Gupta, S.G. Kaler, S. Lutsenko, V. Mittal, M.J. Petris, R. Polishchuk, M. Ralle, M.L. Schilsky, N.K. Tonks, L.T. Vahdat, L. Van Aelst, D. Xi, P. Yuan, D.C. Brady, C.J. Chang, Connecting copper and cancer: from transition metal signalling to metalloplasia, Nat. Rev. Cancer 22 (2) (2022) 102–113.
[9] L. Cui, A.M. Gouw, E.L. LaGory, S. Guo, N. Attarwala, Y. Tang, J. Qi, Y.S. Chen, Z. Gao, K.M. Casey, A.A. Bazhin, M. Chen, L. Hu, J. Xie, M. Fang, C. Zhang, Q. Zhu, Z. Wang, A.J. Giaccia, S.S. Gambhir, W. Zhu, D.W. Felsher, M.D. Pegram, E.A. Goun, A. Le, J. Rao, Mitochondrial copper depletion suppresses triple-negative breast cancer in mice, Nat. Biotechnol. 39 (3) (2021) 357–367.
[10] H. Cai, F. Peng, Knockdown of copper chaperone antioxidant-1 by RNA interference inhibits copper-stimulated proliferation of non-small cell lung carcinoma cells, Oncol. Rep. 30 (1) (2013) 269–275.
[11] P. Tsvetkov, S. Coy, B. Petrova, M. Dreishpoon, A. Verma, M. Abdusamad, J. Rossen, L. Joesch-Cohen, R. Humeidi, R.D. Spangler, J.K. Eaton, E. Frenkel, M. Kocak, S.M. Corsello, S. Lutsenko, N. Kanarek, S. Santagata, T.R. Golub, Copper induces cell death by targeting lipoylated TCA cycle proteins, Science 375 (6586) (2022) 1254–1261.
[12] S. Xu, D. Liu, T. Chang, X. Wen, S. Ma, G. Sun, L. Wang, S. Chen, Y. Xu, H. Zhang, Cuproptosis-associated lncRNA establishes new prognostic profile and predicts immunotherapy response in clear cell renal cell carcinoma, Front. Genet. 13 (2022) 938259.
[13] K. Yin, J. Lee, Z. Liu, H. Kim, D.R. Martin, D. Wu, M. Liu, X. Xue, Mitophagy protein PINK1 suppresses colon tumor growth by metabolic reprogramming via p53 activation and reducing acetyl-CoA production, Cell Death Differ. 28 (8) (2021) 2421–2435.
[14] A.J. Gooding, B. Zhang, L. Gunawardane, A. Beard, S. Valadkhan, W.P. Schiemann, The lncRNA BORG facilitates the survival and chemoresistance of triple-negative breast cancers, Oncogene 38 (12) (2019) 2020–2041.
[15] J.J. Quinn, H.Y. Chang, Unique features of long non-coding RNA biogenesis and function, Nat. Rev. Genet. 17 (1) (2016) 47–62.
[16] S. Agarwal, T. Vierbuchen, S. Ghosh, J. Chan, Z. Jiang, R.K. Kandasamy, E. Ricci, K.A. Fitzgerald, The long non-coding RNA LUCAT1 is a negative feedback regulator of interferon responses in humans, Nat. Commun. 11 (1) (2020) 6348.
[17] I.I. Ne, J.A. Heward, B. Roux, E. Tsitsiou, P.S. Fenwick, L. Lenzi, I. Goodhead, C. Hertz-Fowler, A. Heger, N. Hall, L.E. Donnelly, D. Sims, M.A. Lindsay, Long non-coding RNAs and enhancer RNAs regulate the lipopolysaccharide-induced inflammatory response in human monocytes, Nat. Commun. 5 (2014) 3979.
[18] K.A. Lennox, M.A. Behlke, Cellular localization of long non-coding RNAs affects silencing by RNAi more than by antisense oligonucleotides, Nucleic Acids Res. 44 (2) (2016) 863–877.
[19] Z. Zhang, D. Salisbury, T. Sallam, Long noncoding RNAs in atherosclerosis: JACC review topic of the week, J. Am. Coll. Cardiol. 72 (19) (2018) 2380–2390.
[20] J.W. Shih, W.F. Chiang, A.T.H. Wu, M.H. Wu, L.Y. Wang, Y.L. Yu, Y.W. Hung, W.C. Wang, C.Y. Chu, C.L. Hung, C.A. Changou, Y. Yen, H.J. Kung, Long noncoding RNA LncHIFCAR/MIR31HG is a HIF-1α co-activator driving oral cancer progression, Nat. Commun. 8 (2017) 15874.
[21] G. Chen, D. Lian, L. Zhao, Z. Wang, Q. Wuyun, N. Zhang, The long non-coding RNA T cell leukemia homeobox 1 neighbor enhances signal transducer and activator of transcription 5A phosphorylation to promote colon cancer cell invasion, migration, and metastasis, Bioengineered 13 (4) (2022) 11083–11095.
[22] Q. Chen, L. Zhou, D. Ma, J. Hou, Y. Lin, J. Wu, M. Tao, LncRNA GAS6-AS1 facilitates tumorigenesis and metastasis of colorectal cancer by regulating TRIM14 through miR-370-3p/miR-1296-5p and FUS, J. Transl. Med. 20 (1) (2022) 356.
[23] S. Engebretsen, J. Bohlin, Statistical predictions with glmnet, Clin. Epigenet. 11 (1) (2019) 123.
[24] A.M. Newman, C.L. Liu, M.R. Green, A.J. Gentles, W. Feng, Y. Xu, C.D. Hoang, M. Diehn, A.A. Alizadeh, Robust enumeration of cell subsets from tissue expression profiles, Nat. Methods 12 (5) (2015) 453–457.
[25] P. Jiang, S. Gu, D. Pan, J. Fu, A. Sahu, X. Hu, Z. Li, N. Traugh, X. Bu, B. Li, J. Liu, G.J. Freeman, M.A. Brown, K.W. Wucherpfennig, X.S. Liu, Signatures of T cell dysfunction and exclusion predict cancer immunotherapy response, Nat. Med. 24 (10) (2018) 1550–1558.
[26] Z. Wang, J. Song, N.L.B. Azami, M. Sun, Identification of a novel immune landscape signature for predicting prognosis and response of colon cancer to immunotherapy, Front. Immunol. 13 (2022) 802665.
[27] J. Zhang, D. Velmeshev, K. Hashimoto, Y.H. Huang, J.W. Hofmann, X. Shi, J. Chen, A.M. Leidal, J.G. Dishart, M.K. Cahill, K.W. Kelley, S.A. Liddelow, W. W. Seeley, B.L. Miller, T.C. Walther, R.V. Farese Jr., J.P. Taylor, E.M. Ullian, B. Huang, J. Debnath, T. Wittmann, A.R. Kriegstein, E.J. Huang, Neurotoxic microglia promote TDP-43 proteinopathy in progranulin deficiency, Nature 588 (7838) (2020) 459–465.
[28] A. Bhaduri, E. Di Lullo, D. Jung, S. Müller, E.E. Crouch, C.S. Espinosa, T. Ozawa, B. Alvarado, J. Spatazza, C.R. Cadwell, G. Wilkins, D. Velmeshev, S.J. Liu, M. Malatesta, M.G. Andrews, M.A. Mostajo-Radji, E.J. Huang, T.J. Nowakowski, D.A. Lim, A. Diaz, D.R. Raleigh, A.R. Kriegstein, Outer radial glia-like cancer stem cells contribute to heterogeneity of glioblastoma, Cell Stem Cell 26 (1) (2020) 48–63.e6.
[29] E. Armingol, A. Officer, O. Harismendy, N.E. Lewis, Deciphering cell-cell interactions and communication from gene expression, Nat. Rev. Genet. 22 (2) (2021) 71–88.
[30] J. Kong, H. Lee, D. Kim, S.K. Han, D. Ha, K. Shin, S. Kim, Network-based machine learning in colorectal and bladder organoid models predicts anti-cancer drug efficacy in patients, Nat. Commun. 11 (1) (2020) 5485.
[31] Y. Peng, C. Xu, J. Wen, Y. Zhang, M. Wang, X. Liu, K. Zhao, Z. Wang, Y. Liu, T. Zhang, Fatty acid metabolism-related lncRNAs are potential biomarkers for predicting the overall survival of patients with colorectal cancer, Front. Oncol. 11 (2021) 704038.
[32] N. Liu, X. Chen, J. Ran, J. Yin, L. Zhang, Y. Yang, J. Cen, H. Dai, J. Zhou, K. Gao, J. Zhang, L. Liu, Z. Chen, H. Wang, Investigating the change in gene expression profile of blood mononuclear cells post-laparoscopic sleeve gastrectomy in Chinese obese patients, Front. Endocrinol. 14 (2023) 1049484.
[33] D. Kobak, P. Berens, The art of using t-SNE for single-cell transcriptomics, Nat. Commun. 10 (1) (2019) 5416.
[34] Y. Zhang, M.S. Kim, E.R. Reichenberger, B. Stear, D.M. Taylor, Scedar: a scalable Python package for single-cell RNA-seq exploratory data analysis, PLoS Comput. Biol. 16 (4) (2020) e1007794.
[35] L. Chen, J. Min, F. Wang, Copper homeostasis and cuproptosis in health and disease, Signal Transduct. Targeted Ther. 7 (1) (2022) 378.
[36] T. Ye, L.L. Li, X.M. Peng, Q. Li, CYP1B1-AS1 is a novel biomarker in glioblastoma by comprehensive analysis, Dis. Markers 2021 (2021) 8565943.
[37] P.S. Babich, A.N. Skvortsov, P. Rusconi, N.V. Tsymbalenko, M. Mutanen, L.V. Puchkova, M. Broggini, Non-hepatic tumors change the activity of genes encoding copper trafficking proteins in the liver, Cancer Biol. Ther. 14 (7) (2013) 614–624.
[38] S.A. Choi, J.W. Choi, K.C. Wang, J.H. Phi, J.Y. Lee, K.D. Park, D. Eum, S.H. Park, I.H. Kim, S.K. Kim, Disulfiram modulates stemness and metabolism of brain tumor initiating cells in atypical teratoid/rhabdoid tumors, Neuro Oncol. 17 (6) (2015) 810–821.
[39] S. Zhai, L. Yang, Q.C. Cui, Y. Sun, Q.P. Dou, B. Yan, Tumor cellular proteasome inhibition and growth suppression by 8-hydroxyquinoline and clioquinol requires their capabilities to bind copper and transport copper into cells, J. Biol. Inorg. Chem. : JBIC : Publ. Soc. Biolog. Inorgan. Chem. 15 (2) (2010) 259–269.

[40] T. Ashino, V. Sudhahar, N. Urao, J. Oshikawa, G.F. Chen, H. Wang, Y. Huo, L. Finney, S. Vogt, R.D. McKinney, E.B. Maryon, J.H. Kaplan, M. Ushio-Fukai, T. Fukai, Unexpected role of the copper transporter ATP7A in PDGF-induced vascular smooth muscle cell migration, Circ. Res. 107 (6) (2010) 787–799.
[41] A. Suraweera, A. Duff, M.N. Adams, C. Jekimovs, P.H.G. Duijf, C. Liu, M. McTaggart, S. Beard, K.J. O'Byrne, D.J. Richard, Defining COMMD4 as an anti-cancer therapeutic target and prognostic factor in non-small cell lung cancer, Br. J. Cancer 123 (4) (2020) 591–603.
[42] W. Zhong, H. Zhu, F. Sheng, Y. Tian, J. Zhou, Y. Chen, S. Li, J. Lin, Activation of the MAPK11/12/13/14 (p38 MAPK) pathway regulates the transcription of autophagy genes in response to oxidative stress induced by a novel copper complex in HeLa cells, Autophagy 10 (7) (2014) 1285–1300.
[43] G. Tong, X. Wu, B. Cheng, L. Li, X. Li, Z. Li, Q. Nong, X. Chen, Y. Liu, S. Wang, Knockdown of HOXA-AS2 suppresses proliferation and induces apoptosis in colorectal cancer, Am. J. Tourism Res. 9 (10) (2017) 4545–4552.
[44] H. Shen, L. Wang, Q. Chen, J. Xu, J. Zhang, L. Fang, J. Wang, W. Fan, The prognostic value of COL3A1/FBN1/COL5A2/SPARC-mir-29a-3p-H19 associated ceRNA network in Gastric Cancer through bioinformatic exploration, J. Cancer 11 (17) (2020) 4933–4946.
[45] F. Chen, G. Bai, Y. Li, Y. Feng, L. Wang, A positive feedback loop of long noncoding RNA CCAT2 and FOXM1 promotes hepatocellular carcinoma growth, Am. J. Cancer Res. 7 (7) (2017) 1423–1434.
[46] Y. Jiang, H. Zhang, W. Li, Y. Yan, X. Yao, W. Gu, FOXM1-Activated LINC01094 promotes clear cell renal cell carcinoma development via MicroRNA 224-5p/CHSY1, Mol. Cell Biol. 40 (3) (2020).
[47] Y. Mei, J. Si, Y. Wang, Z. Huang, H. Zhu, S. Feng, X. Wu, L. Wu, Long noncoding RNA GAS5 suppresses tumorigenesis by inhibiting miR-23a expression in non-small cell lung cancer, Oncol. Res. 25 (6) (2017) 1027–1037.
[48] Z. Xue, C. Cui, Z. Liao, S. Xia, P. Zhang, J. Qin, Q. Guo, S. Chen, Q. Fu, Z. Yin, Z. Ye, Y. Tang, N. Shen, Identification of LncRNA Linc00513 containing lupus-associated genetic variants as a novel regulator of interferon signaling pathway, Front. Immunol. 9 (2018) 2967.
[49] J. Chen, Y. Song, M. Li, Y. Zhang, T. Lin, J. Sun, D. Wang, Y. Liu, J. Guo, W. Yu, Comprehensive analysis of ceRNA networks reveals prognostic lncRNAs related to immune infiltration in colorectal cancer, BMC Cancer 21 (1) (2021) 255.
[50] J. Ren, A. Wang, J. Liu, Q. Yuan, Identification and validation of a novel redox-related lncRNA prognostic signature in lung adenocarcinoma, Bioengineered 12 (1) (2021) 4331–4348.
[51] Y. Cheng, X. Wang, P. Qi, C. Liu, S. Wang, Q. Wan, Y. Liu, Y. Su, L. Jin, Y. Liu, C. Li, X. Sang, L. Yang, C. Liu, H. Duan, Z. Wang, Tumor microenvironmental competitive endogenous RNA network and immune cells act as robust prognostic predictor of acute myeloid leukemia, Front. Oncol. 11 (2021) 584884.
[52] R. Li, X. Gao, H. Sun, L. Sun, X. Hu, Expression characteristics of long non-coding RNA in colon adenocarcinoma and its potential value for judging the survival and prognosis of patients: bioinformatics analysis based on the Cancer Genome Atlas database, J. Gastrointest. Oncol. 13 (3) (2022) 1178–1187.
[53] J. Xiao, Y. Liu, J. Yi, X. Liu, LINC02257, an enhancer RNA of prognostic value in colon adenocarcinoma, correlates with multi-omics immunotherapy-related analysis in 33 cancers, Front. Mol. Biosci. 8 (2021) 646786.
[54] X. Wang, J. Zhou, M. Xu, Y. Yan, L. Huang, Y. Kuang, Y. Liu, P. Li, W. Zheng, H. Liu, B. Jia, A 15-lncRNA signature predicts survival and functions as a ceRNA in patients with colorectal cancer, Cancer Manag. Res. 10 (2018) 5799–5806.
[55] G. Lin, H. Wang, Y. Wu, K. Wang, G. Li, Hub long noncoding RNAs with m6A modification for signatures and prognostic values in kidney renal clear cell carcinoma, Front. Mol. Biosci. 8 (2021) 682471.
[56] R. Lin, C. Deng, X. Li, Y. Liu, M. Zhang, C. Qin, Q. Yao, L. Wang, C. Wu, Copper-incorporated bioactive glass-ceramics inducing anti-inflammatory phenotype and regeneration of cartilage/bone interface, Theranostics 9 (21) (2019) 6300–6313.
[57] J.D. Peske, E.D. Thompson, L. Gemta, R.A. Baylis, Y.X. Fu, V.H. Engelhard, Effector lymphocyte-induced lymph node-like vasculature enables naive T-cell entry into tumours and enhanced anti-tumour immunity, Nat. Commun. 6 (2015) 7114.
[58] P. Guha, M. Cunetta, P. Somasundar, N.J. Espat, R.P. Junghans, S.C. Katz, Frontline Science: functionally impaired geriatric CAR-T cells rescued by increased α5β1 integrin expression, J. Leukoc. Biol. 102 (2) (2017) 201–208.
[59] M. Ruella, M. Klichinsky, S.S. Kenderian, O. Shestova, A. Ziober, D.O. Kraft, M. Feldman, M.A. Wasik, C.H. June, S. Gill, Overcoming the immunosuppressive tumor microenvironment of hodgkin lymphoma using chimeric antigen receptor T cells, Cancer Discov. 7 (10) (2017) 1154–1167.
[60] X.Z. Wu, X.Y. Shi, K. Zhai, F.S. Yi, Z. Wang, W. Wang, X.B. Pei, L.L. Xu, Z. Wang, H.Z. Shi, Activated naïve B cells promote development of malignant pleural effusion by differential regulation of T(H)1 and T(H)17 response, Am. J. Physiol. Lung Cell Mol. Physiol. 315 (3) (2018). L443-l55.
[61] S.M. Downs-Canner, J. Meier, B.G. Vincent, J.S. Serody, B cell function in the tumor microenvironment, Annu. Rev. Immunol. 40 (2022) 169–193.
[62] S.A. Lim, J. Kim, S. Jeon, M.H. Shin, J. Kwon, T.J. Kim, K. Im, Y. Han, W. Kwon, S.W. Kim, C. Yee, S.J. Kim, J.Y. Jang, K.M. Lee, Defective localization with impaired tumor cytotoxicity contributes to the immune escape of NK cells in pancreatic cancer patients, Front. Immunol. 10 (2019) 496.
[63] C. Deng, Y. Xu, J. Fu, X. Zhu, H. Chen, H. Xu, G. Wang, Y. Song, G. Song, J. Lu, R. Liu, Q. Tang, W. Huang, J. Wang, Reprograming the tumor immunologic microenvironment using neoadjuvant chemotherapy in osteosarcoma, Cancer Sci. 111 (6) (2020) 1899–1909.
[64] R. Ma, T. Ji, D. Chen, W. Dong, H. Zhang, X. Yin, J. Ma, X. Liang, Y. Zhang, G. Shen, X. Qin, B. Huang, Tumor cell-derived microparticles polarize M2 tumor-associated macrophages for tumor progression, OncoImmunology 5 (4) (2016) e1118599.
[65] C. Xu, S. Sui, Y. Shang, Z. Yu, J. Han, G. Zhang, M. Ntim, M. Hu, P. Gong, H. Chen, X. Zhang, The landscape of immune cell infiltration and its clinical implications of pancreatic ductal adenocarcinoma, J. Adv. Res. 24 (2020) 139–148.
[66] M. Wu, X. Li, R. Liu, H. Yuan, W. Liu, Z. Liu, Development and validation of a metastasis-related gene signature for predicting the overall survival in patients with pancreatic ductal adenocarcinoma, J. Cancer 11 (21) (2020) 6299–6318.
[67] W. Wan, Q. Liu, M.S. Lionakis, A.P. Marino, S.A. Anderson, M. Swamydas, P.M. Murphy, Atypical chemokine receptor 1 deficiency reduces atherogenesis in ApoE-knockout mice, Cardiovasc. Res. 106 (3) (2015) 478–487.
[68] D. Morein, N. Erlichman, A. Ben-Baruch, Beyond cell motility: the expanding roles of chemokines and their receptors in malignancy, Front. Immunol. 11 (2020) 952.
[69] H. Crijns, V. Vanheule, P. Proost, Targeting chemokine-glycosaminoglycan interactions to inhibit inflammation, Front. Immunol. 11 (2020) 483.
[70] A. Mencarelli, L. Graziosi, B. Renga, S. Cipriani, C. D'Amore, D. Francisci, A. Bruno, F. Baldelli, A. Donini, S. Fiorucci, CCR5 antagonism by maraviroc reduces the potential for gastric cancer cell dissemination, Translat. Oncol. 6 (6) (2013) 784–793.
[71] B.D. Jenkins, R.N. Martini, R. Hire, A. Brown, B. Bennett, I. Brown, E.W. Howerth, M. Egan, J. Hodgson, C. Yates, R. Kittles, D. Chitale, H. Ali, D. Nathanson, P. Nikolinakos, L. Newman, M. Monteil, M.B. Davis, Atypical chemokine receptor 1 (DARC/ACKR1) in breast tumors is associated with survival, circulating chemokines, tumor-infiltrating immune cells, and African ancestry, Cancer Epidemiol. Biomark. Prevent.: A Publ. Am. Asso. Cancer Res. Cosponsor. Am. Soc. Prevent. Oncol. 28 (4) (2019) 690–700.
[72] J.C. Martin, C. Chang, G. Boschetti, R. Ungaro, M. Giri, J.A. Grout, K. Gettler, L.S. Chuang, S. Nayar, A.J. Greenstein, M. Dubinsky, L. Walker, A. Leader, J. S. Fine, C.E. Whitehurst, M.L. Mbow, S. Kugathasan, L.A. Denson, J.S. Hyams, J.R. Friedman, P.T. Desai, H.M. Ko, I. Laface, G. Akturk, E.E. Schadt, H. Salmon, S. Gnjatic, A.H. Rahman, M. Merad, J.H. Cho, E. Kenigsberg, Single-cell analysis of Crohn's disease lesions identifies a pathogenic cellular module associated with resistance to anti-TNF therapy, Cell 178 (6) (2019) 1493, 508.e20.
[73] W.C. Liao, H.R. Yen, C.K. Liao, T.J. Tseng, C.T. Lan, C.H. Liu, DSE regulates the malignant characters of hepatocellular carcinoma cells by modulating CCL5/CCR1 axis, Am. J. Cancer Res. 9 (2) (2019) 347–362.
[74] G. Stoll, J. Pol, V. Soumelis, L. Zitvogel, G. Kroemer, Impact of chemotactic factors and receptors on the cancer immune infiltrate: a bioinformatics study revealing homogeneity and heterogeneity among patient cohorts, OncoImmunology 7 (10) (2018) e1484980.
[75] J.L.F. Teh, A.E. Aplin, Arrested developments: CDK4/6 inhibitor resistance and alterations in the tumor immune microenvironment, Clin. Cancer Res. : Off. J. Am. Asso. Cancer Res. 25 (3) (2019) 921–927.
[76] J. Shi, D. Jiang, S. Yang, X. Zhang, J. Wang, Y. Liu, Y. Sun, Y. Lu, K. Yang, LPAR1, correlated with immune infiltrates, is a potential prognostic biomarker in prostate cancer, Front. Oncol. 10 (2020) 846.
[77] H. J, Y. K, L. M, E. W, K. R, Mouse models for colorectal cancer, Oncogene 18 (1999).

[78] M.S. Peter, W. Rachel Palmieri, S.I. Edwin, B. Yonathan, I.A. Christopher, K. Peter, J.H. Rayjean, A.S. Thomas, S.W. John, P. Paul, E.H. Brian, B.G. Stephen, J. H. David, E.G. Judy, D.J. Amit, M. Kevin, F.E. Doug, E. Ros, K.-J. Zsofia, M. Kenneth, A.D. Jennifer, M.S. Joellen, A cross-cancer genetic association analysis of the DNA repair and DNA damage signaling pathways for lung, ovary, prostate, breast, and colorectal cancer, Cancer Epidemiol. Biomarkers Prev. 25 (2015).
[79] I. Hiroyuki, S. Atsushi, K. Toshiyuki, S. Hiroki, K. Michihiro, A. Tomohiro, K. Hirotaka, K. Shuhei, K. Yoshiaki, K. Takeshi, F. Hitoshi, M. Yukiko, K. Eiichi, O. Eigo, CACNA2D1 regulates the progression and influences the microenvironment of colon cancer, J. Gastroenterol. (2024).
[80] L. Anny-Claude, F. Shuling, N. Hikaru, M.L. Antonio, M. Jael, S.H. Roland, C. Jonas, N. Asma, A.P. Charles, CXADR-like membrane protein regulates colonic epithelial cell proliferation and prevents tumor growth, Gastroenterology 166 (2023).
[81] W. Zhenzhen, Z. Xuanxuan, A. Yunhe, M. Kaiyue, X. Ruixin, Y. Gaoqi, D. Junfeng, C. Zhiyong, Z. Zijing, S. Guizhi, D. Xiang, W. Meng, J. Bing, Z. Peng, L. Jinbo, B. Pengcheng, CLMP is a tumor suppressor that determines all-trans retinoic acid response in colorectal cancer, Dev. Cell 58 (2023).
[82] Z. Hongkai, Z. Chuanzhao, H. Baohua, GTF2IRD1 overexpression promotes tumor progression and correlates with less CD8+ T cells infiltration in pancreatic cancer, Biosci. Rep. 40 (2020).
[83] N. Sho, M. Takaaki, K. Yuta, S. Kuniaki, T. Taro, K. Kensuke, N. Miwa, O. Yushi, K. Yousuke, I. Shuhei, E. Hidetoshi, S. Keishi, M. Koshi, GTF2IRD1 on chromosome 7 is a novel oncogene regulating the tumor-suppressor gene TGFβR2 in colorectal cancer, Cancer Sci. 111 (2019).